The X-ray Emission from Cloud Collisions in O-Star Winds

A. Feldmeier, A. Pauldrach, and J. Puls

Univ. Sternwarte, Scheinerstr. 1, 81679 München, Germany

Abstract. We propose that collisions of gas clouds in O-star winds generate the observed X-ray emission, $L_X \simeq 10^{-7} L_{\rm Bol}$. Fast cloudlets at roughly the stationary wind density collide with slow, massive, and highly compressed clouds. We discuss the origin and dynamics of the clouds as result of the line-driven instability, and the properties of X-ray emission from the strong reverse shock generated in a collision.

1. Introduction

Shortly after the detection of O stars as X-ray sources (Harnden et al. 1979; Seward et al. 1979), Lucy & White (1980) and Lucy (1982) proposed phenomenological models where the line-driven instability (Lucy & Solomon 1970) causes chaotic, hypersonic motions in the dense winds from these stars, with strong X-ray emission from the accompanying shocks.

In these models, fast blobs of dense gas are radiatively driven through slow, ambient gas which is shadowed by the blobs, and is not itself driven. The blobs overtake the slow gas, and *accelerate* it in a *forward* shock. By contrast, Owocki et al. (1988) found that shadowing is only a secondary effect, i.e., forward shocks are weak, and that instead the distinct feature of wind dynamics is fast streams of thin gas which are strongly accelerated over rather large distances ($\lesssim 1R_*$), and then *decelerated* and highly compressed in a *reverse* shock.

However, these quasi-steady, rarefied streams are inefficient X-ray emitters when being shock heated, and produce fluxes which fall about two orders of magnitude below the observed ones.

Occasionally, however, much stronger fluxes can result when tiny cloudlets at roughly stationary wind density collide with a pronounced cloud (Feldmeier et al. 1997). These cloudlets form in the 'shadowed' gas ahead of pronounced clouds, and are strongly accelerated through empty intercloud space until they eventually ram into the next outer, pronounced cloud; the situation is sketched in Fig. 1. By introducing stochastic perturbations at the wind base, a wealth of such cloudlets is generated at some height in the wind, and the *average* emission from their X-ray flashes can indeed match the observed flux.

Notice that, while all hydrodynamic wind simulations so far have assumed one-dimensional, spherical symmetry, the true lateral length scale of wind structure is expected to be small due to photospheric turbulence and/or sound emission, which plausibly act as the seed perturbations for the line-driven instability,

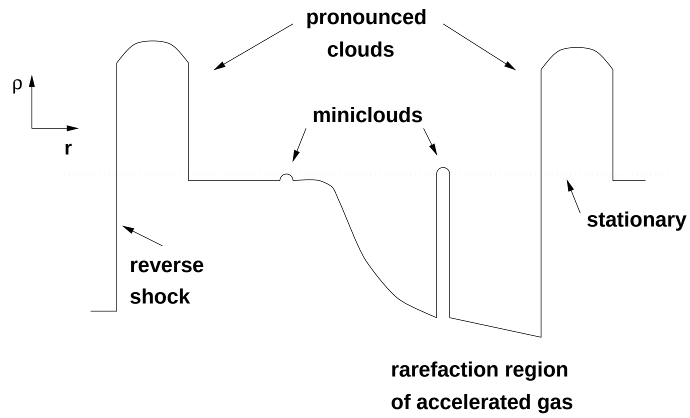

Figure 1. The radial density stratification which develops from the line-driven instability.

and due to Kelvin-Helmholtz or Rayleigh-Taylor induced mixing in the wind itself. We shall therefore always speak of wind *clouds,* rather than shells.

2. Wind Dynamics

The 'building blocks' of fully developed wind structure from the line-driven instability are then: (1) broad rarefaction regions over which the gas is highly accelerated; (2) strong reverse shocks, in which the gas is decelerated again, and accumulates onto overdense, pronounced clouds; and (3) fast cloudlets. How do these structures evolve?

2.1. Rarefaction Regions and Reverse Shocks

These together are the primary feature of unstable growth. Within a localized, accidental elevation of the wind velocity law ($v'' < 0$, where primes indicate spatial differentiation), the optical depth drops. This can be seen from including curvature terms in the Sobolev optical depth. The line force rises, enhancing the elevation, and the optical depth drops further, i.e., one has an amplification cycle. Furthermore, when the perturbation amplitude has grown sufficiently large, fast gas in the crest overtakes slow gas ahead (before the crest itself propagates significantly), i.e., the elevations *break* into a sawtooth of broad accelerating regions and decelerating reverse shocks.

To achieve large velocity jumps, $v_{\rm j} \gg v_{\rm th}$ (with $v_{\rm th}$ the thermal speed), the elevations have to extend over many Sobolev lengths, $L = v_{\rm th}/v'$. While such broad perturbations grow much more slowly than short-scale perturbations $< L/2$ (Owocki & Rybicki 1984), as long as $\lambda/L \lesssim 100$ at the sonic point they are still able to grow by many e-folds out to a few stellar radii. Short-scale, noisy structure at $v_{\rm j} \simeq v_{\rm th}$ is then expected to be superimposed on such a 'coherent' tilt of the thermal band.

The velocity jumps at reverse shocks can be estimated as follows. The instability steepens or tilts the thermal-velocity band of the wind until the band becomes optically thin, hence no further deshadowing is possible, and the instability ceases. For a single line of optical depth $\tau > 1$, the line force rises by a factor of $\sim\tau$ when the gas becomes optically thin (neglecting a term $1 - e^{-\tau}$), and, for an ensemble of weak and strong lines with an opacity distribution after Castor et al. (1975) which becomes optically thin, the total line force raises by a factor of $\sim\tau_{\rm m}^{\alpha}$. Here, $\tau_{\rm m}$ is the optical depth of the strongest line present, and $\alpha = 2/3$ typically. Assuming quasi-stationarity, $vv' \equiv g$, one has for such an ensemble

$$\frac{v_{\rm j}}{v_\infty} \simeq \frac{\sqrt{\tau_{\rm m}^{\alpha} R_* h}}{r}, \tag{1}$$

where h is the extent of the optically thin, accelerating region. The broadest elevations which are still able to grow into saturation have $h \lesssim 1 R_*$ at a few stellar radii. Furthermore, simulations so far have been for winds with $\tau_{\rm m} \simeq 100$. This implies $v_{\rm j} \lesssim v_\infty$ at the strongest shocks, as is confirmed by the simulations.

2.2. Pronounced Clouds

Assuming efficient radiative cooling, and therefore isothermal shocks, the shock-compression ratio is $\lesssim (v_\infty/a)^2 \simeq (2000/20)^2 = 10^4$. If the gas at the foot-point of a rarefaction region has stationary density ρ_0 (after Castor et al. 1975 or Pauldrach et al. 1986), the strong acceleration should stretch it to have a preshock density of $\rho_0/\tau_{\rm m}^{\alpha} \simeq \rho_0/20$, which would imply cloud overdensities of $\sim$1.5 dex above stationary wind values. The true preshock density, however, is even smaller, since gas is fed continuously into pronounced clouds and trapped there, i.e., the intercloud space becomes gradually depleted. In numerical simulations, the densities of pronounced clouds are therefore typically 1.5 to 2 dex above stationary values.

In Fig. 2, perturbations are introduced at the subsonic wind base to trigger unstable growth, and the origin of the pronounced clouds can be traced back to the sonic point at $1.02 R_*$, and even somewhat below. Some dynamical details on the formation of such deep cloud seeds, especially their role in adjusting to the correct mass-loss rate which can be driven by the photospheric radiation field, are discussed by Owocki (1990). Since the clouds form in dense surroundings, any momentum they gain is preferentially used to increase the cloud's mass, not its speed: initially, the cloud grows by stopping fast, inner gas. This pushes it into outer gas, which it collects up, whereby the cloud is decelerated again.

Since these clouds are the most pronounced structures in the wind, their ultimate decay determines the return of the wind to stationary conditions. In particular, the clouds re-expand due to internal pressure, and it is estimated that by $50 R_*$ the wind density is approximately homogeneous again. This is confirmed by the simulations.

2.3. Miniclouds

The time interval between the passage of two pronounced clouds corresponds to the largest base-perturbation periods, which in turn should be close to the acoustic cutoff period (Owocki 1990). If shorter periods are also present, they could give rise to a rather different population of *fast miniclouds.* The latter

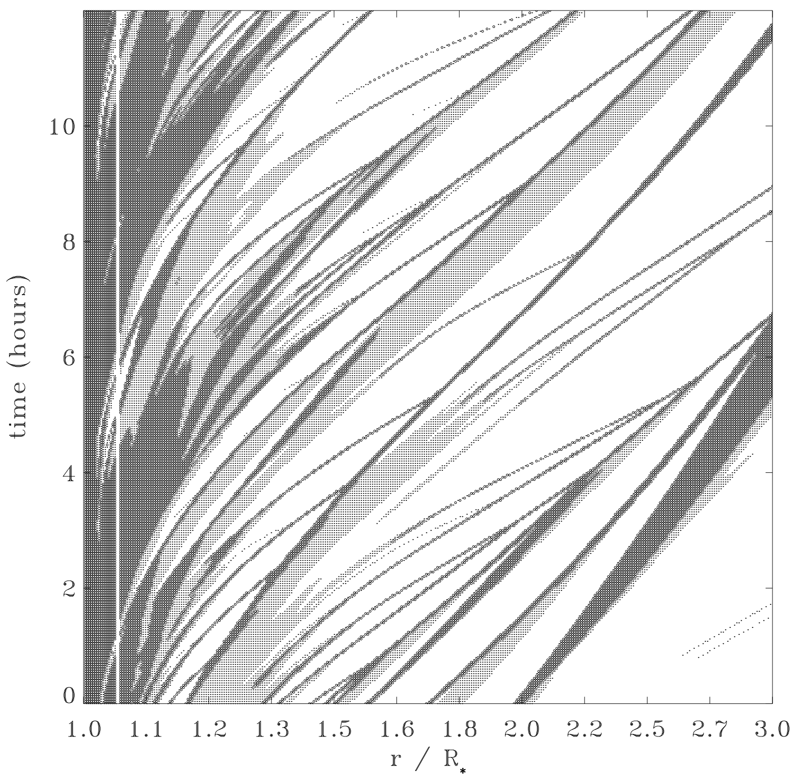

Figure 2. Evolution of the wind density in a simulation of an unstable O-supergiant wind. Grey indicates densities between $\rho_0/3$ and ρ_0, where ρ_0 is the stationary wind density; black indicates densities $\geq \rho_0$. (The stripe at $1.05R_*$ is artificial.) Notice that miniclouds become denser during their propagation.

form in the dense gas ahead of a pronounced cloud, which has not yet fed into the next outer pronounced cloud, and are accelerated to large velocities through the void intercloud space ahead of them. The maximum line force possible is that on optically thin gas. However, the cloudlets are far from being optically thin! Instead, Fig. 3 shows that their optical depth often lies between 10 and 100 (where the pronounced clouds have $\tau \simeq 1000$, and the stationary wind $\tau \simeq 100$). Consequently, the cloudlets are also pushed by stopping thin, fast, inner gas, which itself is continuously ablated from dense gas ahead of a pronounced cloud.

Since most hot-star wind simulations so far (Owocki et al. 1988; Owocki 1991; Feldmeier 1995) studied the response of the wind to a *coherent,* single-period perturbation, they overlooked the dynamical importance of these miniclouds. (Actually, however, a few miniclouds even show up in coherent models, which is due to wave steepening and the occurence of subharmonics of the basic perturbation period.) A more natural choice for possible triggering perturba-

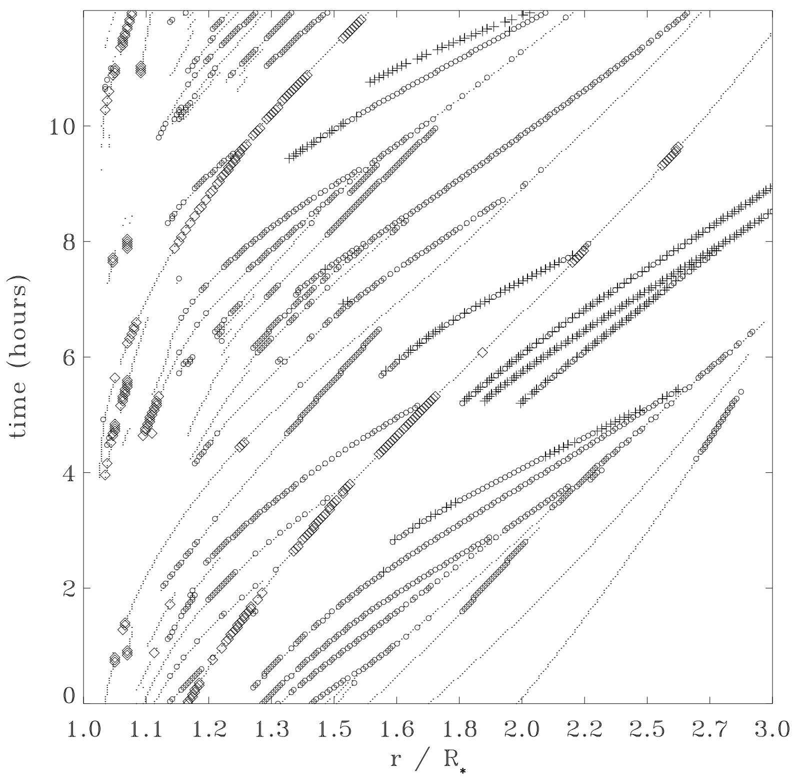

Figure 3. Maximum line optical depths τ_m of the clouds from Fig. 2. For $(\times, +, \circ, \cdot, \diamond)$, the optical depth is larger than $(10^{-1}, 1, 10, 10^2, 10^3)$, respectively.

tions at the wind base is photospheric turbulence and/or stochastic sound emission, both of which show a multitude of excited periods. Actually, Fig. 2 is for a simple model of stochastic sound emission, namely a tunable sound wave. The case of photospheric (Langevin) turbulence gives comparable results.

3. X-ray Emission from Cloudlet-Cloud Collisions

3.1. Luminosity

The energy thermalized in the collision of a cloudlet with the next outer, pronounced cloud is radiated away, predominantly in X-rays. We estimate the luminosity of such a collision. The energy density of hot gas is

$$e = \frac{3}{2} nkT = \frac{1}{2} \rho v_\mathrm{j}^2, \tag{2}$$

where the energy of cold ($\lesssim T_{\rm eff}$) wind gas is neglected; $v_{\rm j}$ is now meant to be the velocity difference of a cloudlet before and after collision. With a relative velocity $v_{\rm p}$ between cloudlet and pronounced cloud, the heating rate, and therefore X-ray luminosity, is

$$L_{\rm X} = 4\pi r^2 v_{\rm p} \cdot e. \tag{3}$$

For an adiabatic shock, $v_{\rm j} = 3v_{\rm p}/4$, and introducing the mechanical wind luminosity, $L_{\rm w} = \frac{1}{2}\dot{M}v_\infty^2$, gives

$$\frac{L_{\rm X}}{L_{\rm w}} = \frac{9}{16}\,\frac{v_\infty}{v_0}\,\frac{\rho_{\rm h}}{\rho_0}\left(\frac{v_{\rm p}}{v_\infty}\right)^3, \tag{4}$$

where $\rho_{\rm h}$ explicitly refers to the density of hot gas. No significant X-ray emission is expected from below $2R_*$ where wind structures still grow, and one can assume $v_\infty/v_0 \simeq 1$.

The efficiency of minicloud collisions in generating X-rays is then based on $\rho_{\rm h}/\rho_0 \simeq 1$. Figure 2 shows that miniclouds indeed have densities which are close to stationary values; Figs. 9 and 15 of Feldmeier et al. (1997) show that the same is true (within $\pm$ 1 dex) for X-ray emitting gas.

One major reason that miniclouds stay at large densities is that they are optically thick, and gain momentum through stopping inner gas. The driving force is then a *surface* force, not a volume or body force, wherefore accelerated fluid parcels do *not* stretch in accordance with their actual velocity (e.g., by the above factor of 20).

Finally, for such optically thick cloudlets, $v_{\rm j}$ is usually somewhat smaller than the estimate given by eqn. (1) for optically thin gas driven at maximum acceleration. Typically, $v_{\rm j} \simeq v_\infty/3$ for the cloudlets, resulting in a temperature $T = 10^7$ K when thermalized.

3.2. Loci of X-ray Emission; Variability

In numerical simulations, the last cloudlet-cloud collisions occur at $\lesssim 10R_*$. The outer radius for significant X-ray emission therefore lies well below those radii where the wind returns to stationary conditions ($\sim 50R_*$). For simulations of the O9 supergiant ζ Ori, 90% of the emergent X-ray flux (i.e., after reabsorption in the cold wind) stems from below $10R_*$, and 99.7% from below $30R_*$.

The X-ray emission from the 'standard' O4 supergiant ζ Pup is therefore puzzling. For this star, Hillier et al. (1993) conclude that X-rays below 0.3 keV should be emitted from above $30R_*$, since helium recombination enhances the wind opacity enormously.

Furthermore, from Fig. 2, at most one or two cloud collisions occur at any time over the full radial wind range. This leads to strong variability of the X-ray flux within ± 1 dex around the mean. By contrast, the observed flux variations for ζ Ori are below a few per cent.

One obvious explanation is that spherical symmetry is an invalid assumption in the presence of stochastic base perturbations. Instead, photospheric turbulence and/or stochastic sound emission should generate a multitude of independent, more or less radial wind cones of small opening angle, each with its own cloud collisions taking place. A few thousand such cones would guarantee the observed flux constancy. This lies well below the number of 10^5 coherent patches of the photosphere which are expected for an assumed coherence time of 5000 s in the simulations.

4. Outlook

Cloud formation is a natural consequence of the line-driven instability of O-star winds, and, at least for the one star ζ Ori considered so far, mutual cloud collisions can reproduce the observed X-ray flux. Work in different directions is required now:

(1) A systematic study over the whole O-type spectral class, and from main-sequence stars to supergiants, is needed. Can the observed flux levels be always matched? Can the relation $L_{\mathrm{X}} \sim L_{\mathrm{Bol}}$, possibly extended by other stellar or wind parameters, be understood? Can the breakdown of this relation around spectral type B2 V (Cassinelli et al. 1994) be understood?

(2) An improved numerical technique is needed to simulate cloud collisions, which are presently only resolved by a few spatial grid points. Cooper (1994) noticed that already the resolution of radiative cooling zones is problematic in the simulations. Cloud collisions occur on length scales which are yet another order of magnitude shorter.

Acknowledgments. I thank Drs. S. Owocki, C. Norman, R. Kudritzki, R. Palsa, U. Springmann, L. Lucy, and A. Fullerton for interesting discussions, and Ms. C. Brunner from Leibniz Rechenzentrum for technical assistance. This work was supported by DFG grants Pa 477/1-2 and 1-3, and BMBF grant 50 OR 9304.

References

Cassinelli, J. P., Cohen, D. H., MacFarlane, J. I., Sanders, W. T., Welsh, B. Y., 1994, ApJ, 421, 705

Castor, J. I., Abbott, D. C., Klein, R. I., 1975, ApJ, 195, 157

Cooper, R. G., 1994, PhD Thesis, University of Delaware

Feldmeier, A., 1995, A&A, 299, 523

Feldmeier, A., Puls, J., Pauldrach, A. W. A., 1997, A&A, 322, 878

Harnden, F. R., Branduardi, G., Elvis, M., et al., 1979, ApJ, 234, L51

Hillier, D. J., Kudritzki, R. P., Pauldrach, A. W. A., et al., 1993, A&A, 276, 117

Lucy, L. B., 1982, ApJ, 255, 286

Lucy, L. B., Solomon, P. M., 1970, ApJ, 159, 879

Lucy, L. B., White, R. L., 1980, ApJ, 241, 300

Owocki, S. P., 1990, IAU Symp. 143, 155

Owocki, S. P., 1991, in Stellar Atmospheres: Beyond Classical Models (NATO ASI Series C341), eds. L. Crivellari, I. Hubeny & D. G. Hummer (Kluwer, Dordrecht), p. 235

Owocki, S. P., Rybicki, G. B., 1984, ApJ, 284, 337

Owocki, S. P., Castor, J. I., Rybicki, G. B., 1988, ApJ, 335, 914

Pauldrach, A., Puls, J., Kudritzki, R. P., 1986, A&A, 164, 86
Seward, F. D., Forman, W. R., Giacconi, R., et al., 1979, ApJ, 234, L55

Discussion

Kaper: At what depth in your model does the wind become optically thick to soft X-rays?
Feldmeier: 3–4R_* for intermediate energies ($\sim$1 keV), and the effective X-ray photosphere is at 2–3R_*. For all the examples I showed, the X-ray photosphere is below the cloud–cloud collisions.
Owocki: Surely that must depend on the mass-loss rate; I seem to remember from Hillier et al. that at 1 keV the X-ray photosphere for ζ Pup was at 10R_*?
Feldmeier: Yes, that's a very strange point; in Hillier's model, nearly all the X-rays are re-absorbed. Leon Lucy also asked me to make a comparison between my results and his model, and I found that in his model also 99.9% of X-rays should be re-absorbed in the wind, whereas in our models the figure is only 90%. I asked Ralf Palsa, who analysed our Rosat dataset of 42 O-type stars, what number he got, and it's remarkable how close it usually is to 90%. So, I think the Hillier case was exceptional because he had helium recombining in the wind, and ζ Pup is one of very few stars where this occurs. I would make the claim that, in general, X-ray absorption in stellar winds has previously been overestimated.
Owocki: Okay, but I thought that in the Hillier model the non-helium absorption at 10R_* was still considerable at 1 keV?
Feldmeier: No, it was was mostly helium. It's also true that the present model would not work for ζ Pup.